SIMPLIFIED SEISMIC ANALYSIS OF LOCK GATES

by

Loïc Buldgen[1], Hervé Degée[2], Hervé Le Sourne[3] and Philippe Rigo[4]

ABSTRACT

The paper deals with the seismic design of lock gates. When such structures are submitted to an earthquake, the water contained in the chamber is responsible for an additional hydrodynamic pressure acting on the gate. This one is the sum of three different parts, respectively called the convective, rigid and flexible contributions. The two first ones have already been extensively studied in the literature, but the flexible part is more difficult to assess as it is largely influenced by the coupling occurring between the fluid and the gate. To overcome this difficulty, it is of course possible to use finite elements software, but doing so is not always convenient. This is why some research have been undertaken to provide a rapid way for approximating the flexible pressure on lock gates. This is achieved by applying the analytical approach that is shortly presented in this paper. As a matter of validation, the results obtained through this simplified procedure are compared to numerical solutions. The agreement between both of them is found to be satisfactory.

1. INTRODUCTION

When a lock chamber is submitted to a longitudinal ground acceleration, an additional hydrodynamic pressure is applied on the gates because the water confined between the downstream and upstream gates is also put into motion. The resulting total pressure is known to have the three following contributions:

- The *convective* part associated to the sloshing appearing at the free surface of the lock chamber. Most of the time, this contribution is negligible, as the lock chamber is quite long. Accounting for the convective pressure is more relevant for smaller reservoirs, where the liquid is strongly confined.
- The *rigid impulsive* part, which is derived by assuming that the gates are rigid and therefore moving in unison with the ground. This is typically the pressure that is used for designing concrete dams for example.
- The *rigid flexible* part, which is coming from the own vibrations of the gates during the earthquake. These ones also produce an additional water pressure that would not be present if the gate were perfectly rigid.

The two first parts have already been extensively investigated in the literature. Many improved developments are nowadays available since the pioneer work of Westergaard [5], such as those perfomed by Haroun [1], Housner [2], Ibrahim [3] or Epstein [4] amongst others. All these authors provide various analytical formulae for deriving the rigid and convective pressures.

However, assessing the third contribution is more difficult. This is due to the coupling taking place between the structure and the fluid. Indeed, the flexible pressure is directly influenced by the vibrations of the gate, which also has an influence on the motion of the structure. It is not easy to have a simplified analytical treatment of such an fluid-structure interaction problem. For this reason, an alternative solution is to perform a numerical investigation of this phenomenon by using finite elements software.

Nowadays, it is evident that such numerical tools constitute a precious help for engineers by allowing them to solve a great number of technical problems. Nevertheless, finite elements also have some practical drawbacks, in particular for performing coupled fluid-structure analyses. This is briefly explained hereafter:

- Having a proper modeling of the fluid, the structure and the coupling occurring between them is not easy to achieve. Developing a consistent model is not straightforward, one of the main problem being the leakages appearing during the simulation. This task is quite arduous and may therefore

[1] FRIA PhD Student, University of Liège, Belgium, L.Buldgen@ulg.ac.be
[2] Associate Professor, Hasselt University, Belgium
[3] Professor, Institut Catholique d'Arts et Métiers de Nantes, France
[4] Professor, University of Liège, Belgium

turns out to be time demanding. Moreover, the work has to be achieved by engineers that are already used with such particular finite elements approaches.

- Simulating the interaction between the liquid and the structure requires both of them to be represented. Doing so may have a considerable influence on the size of the model, in particular for lock chambers that are already quite large.
- The calculation time is often prohibitive, due to the size of the model and the total duration of the earthquake.

The non-exhaustive list presented here above clearly shows that having a purely numerical approach of the seismic response of lock gates is not a convenient way of working at the pre-design stage of such structures. As a consequence, another approach is required to include the effects of earthquakes in the early phases of design. This is particularly true when building new locks in sensible areas like the east side of America for example. The goal of this paper is therefore to present a new simplified methodology that can be used to overcome this difficulty.

2. SIMPLIFIED ANALYTICAL METHODOLOGY

Let us now have a brief presentation of the mathematical procedure leading to a rapid prediction of the flexible pressure acting on a lock gate. This will be achieved by deriving first the vibration properties of the structure. The results will then be used within a dynamic analysis to investigate the effects of an earthquake.

2.1. Properties of the Gate

In this article, we consider a basic rectangular chamber bounded by two identical upstream and downstream lock gates having a width l and a height H, as depicted on Figure 1. The total length of the lock is L and the water level is denoted by h_s.

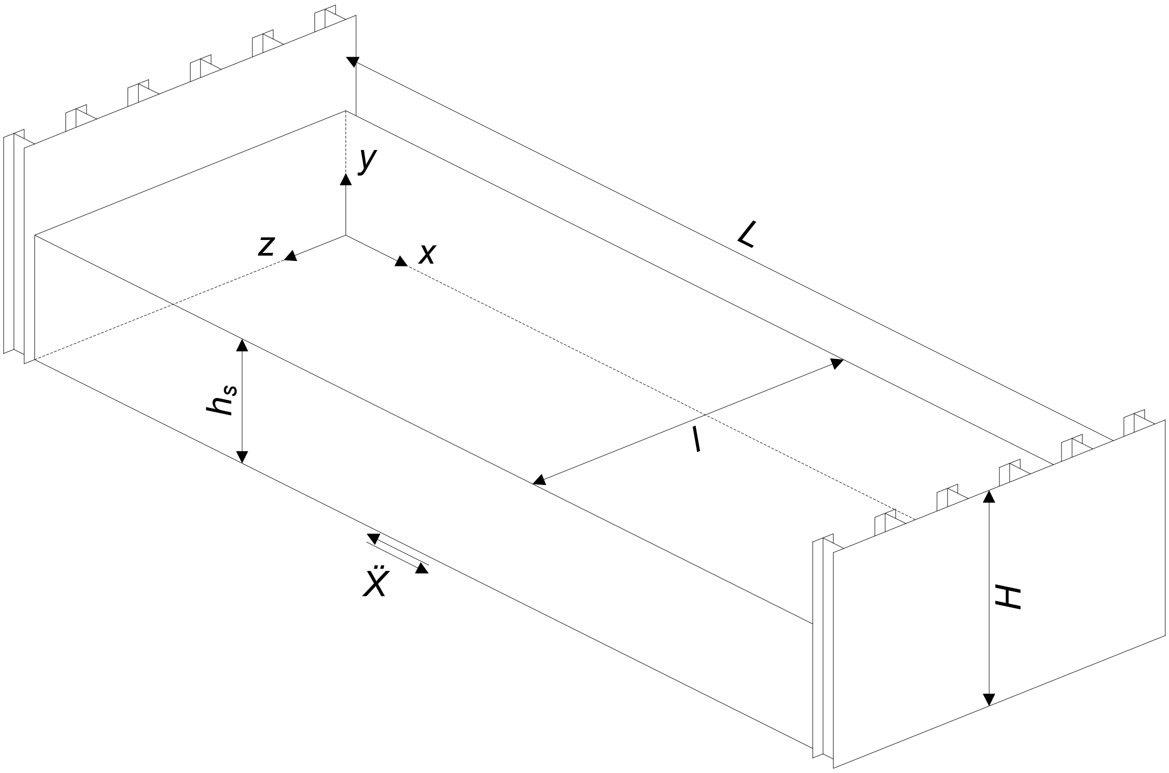

Figure 1: Main Parameters Characterizing the Lock Chamber

During a seismic event, this configuration is submitted to three different accelerations acting along the x, y and z axes. In this paper, only the longitudinal acceleration $\ddot{X}$ is considered, but the methodology exposed here may be easily extended to the vertical and transversal ones. Nevertheless, as the stiffness of the gate is quite important along the y and z directions, it is worth noting that the flexible contributions of the accelerations acting along these two axes are usually quite negligible in comparison with the rigid impulsive ones.

The gate is assumed to have a single plating reinforced by an orthogonal stiffening system (Figure 2a) made of vertical and horizontal elements. The first ones are called the frames and oriented along the y axis (Figure 2b), while the second ones are called the girders and oriented along the z axis (Figure 2c). Some additional horizontal and/or vertical smaller stiffeners may also be present, mainly to provide the local buckling of the plating. All these elements have a T-shaped cross-section (Figure 2d), with a web height h_w and a flange width h_f. The associated thicknesses are respectively t_w and t_f, while the notation t_p is used for the plating.

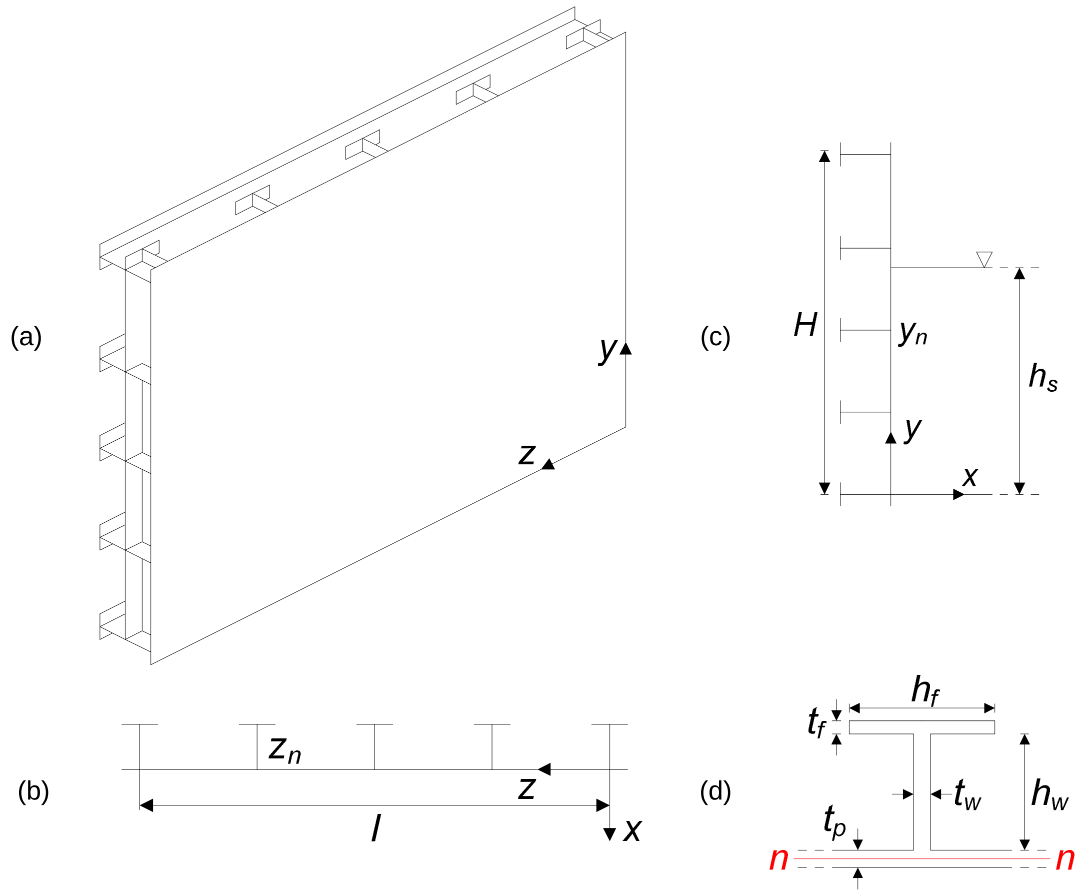

Figure 2: Main Parameters Characterizing the Lock Gate

Regarding the boundary conditions for the analytical model, we suppose that the gate is simply supported in $z = 0$ and $z = l$, while the bottom and top edges are free to move.

2.2. Free Vibration Analysis

Let us start by finding first the modal properties of the dry structure. The aim is now to derive an analytical approximation of the natural frequencies ω_i and modes shapes δ_i characterizing the gate by assuming that this one is not surrounded by water. This can be achieved by applying the Rayleigh-Ritz method, as described by Shames [6]. Some examples of this procedure are given in references [7], [8] and [9] for plates with different boundary conditions.

The basis of the Rayleigh-Ritz method is to make the hypothesis that the modes shapes δ_i may be decomposed into a set of admissible functions ψ_j. These latter are arbitrarily chosen but they have to satisfy the boundary conditions exposed here above. With this assumption, we may write:

$$\delta_i(y,z) = \sum_{j=1}^{M} v_{ji}\psi_j(y,z) \tag{1}$$

where M is the total number of functions used for estimating δ_i. Of course, the approximation will be more refined for very high values of M, but this has the main drawback to make the analytical treatment more difficult to follow. In (1), the coefficients v_{ji} are unknown and will be fixed as explained hereafter.

In this paper, we propose to chose ψ_j by combining some functions f_j and g_j respectively characterizing the vibrations of the main horizontal and vertical stiffening elements reinforcing the gate. In other words, we suppose that:

$$\psi_j(y,z) = f_j(y)g_j(z) \tag{2}$$

Furthermore, as the girders are simply supported in $z = 0$ and $z = l$, it seems reasonable to chose g_j as being the eigenmodes of a doubly supported beam with a span l (Figure 3a). Similarly, as the gate is free along its top and bottom edges, the frames can be supposed to vibrate as free-free beams and it may be therefore convenient to choose f_j as being the associated eigenmodes (Figure 3b).

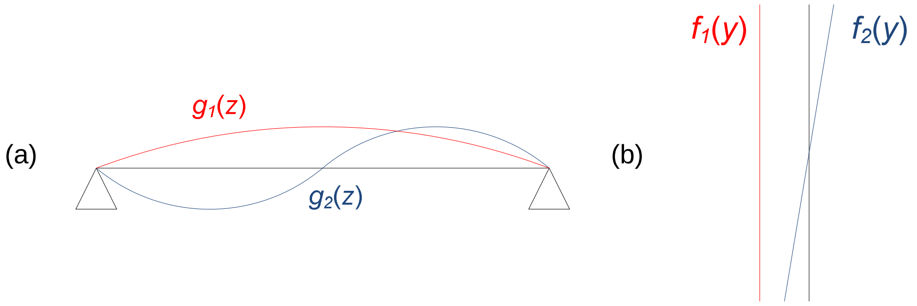

Figure 3: Two First Eigenmodes for a Doubly Supported Beam and for a Free-Free Beam

The analytical derivation of f_j and g_j will not be performed in this paper as many references are available in the literature. The corresponding mathematical expressions are detailed by Leissa [10] for example and will not be recalled here. If we introduce them in (1), we finally get an approximate decomposition of the eigenmodes characterizing the dry structure. The next step is then to determine the unknown coefficients v_{ji}.

This operation has to be performed by evaluating the internal and kinetic energies U and T characterizing the free vibrations of the structure. If we follow the same assumptions than Shames [6], U may be seen as the sum of two different contributions U_p and U_r respectively coming from the plating and the reinforcing system. These ones are given by:

$$\begin{aligned} U_p &= \frac{D}{2}\iint_A \left(\left(\frac{\partial^2\delta_i}{\partial y^2}\right)^2 + \left(\frac{\partial^2\delta_i}{\partial z^2}\right)^2 + 2\nu\frac{\partial^2\delta_i}{\partial y^2}\frac{\partial^2\delta_i}{\partial z^2} + 2(1-\nu)\left(\frac{\partial^2\delta_i}{\partial y\partial z}\right)^2\right)dydz \\ U_r &= \sum_n \frac{EI_{h,n}}{2}\int_0^l \left[\frac{\partial^2\delta_i}{\partial z^2}(y_n,z)\right]^2 dz + \sum_n \frac{EI_{v,n}}{2}\int_0^H \left[\frac{\partial^2\delta_i}{\partial y^2}(y,z_n)\right]^2 dy \end{aligned} \tag{3}$$

where ν and E are respectively the Poisson ratio and Young modulus. The plate is characterized by its surface A and bending flexibility D. The inertias of the horizontal and vertical reinforcing elements are designated by $I_{h,n}$ and $I_{v,n}$ respectively, while y_n and z_n denotes the discrete locations occupied by the frames and the girders.

In a similar way, the kinetic energy $\omega_i^2 T$ due to the vibrations of the gate is also to be found by summing up the two contributions $\omega_i^2 T_p$ and $\omega_i^2 T_r$. According to Shames [6], we have:

$$\begin{aligned} T_p &= \frac{\rho t_p}{2}\iint_A \delta_i^2(y,z)dydz \\ T_r &= \sum_n \frac{\rho A_{h,n}}{2}\int_0^l \delta_i^2(y_n,z)dz + \sum_n \frac{\rho A_{v,n}}{2}\int_0^H \delta_i^2(y,z_n)dy \end{aligned} \tag{4}$$

where ρ is the mass density, while $A_{h,n}$ and $A_{v,n}$ respectively denote the cross-sectional areas of the girders and the frames. If we further introduce *(1)* in *(3)* and *(4)*, it is possible to get a matrix formulation for T and U. This operation is quite fastidious, so we will not provide here the detailed derivation. If $\boldsymbol{v}_i$ is the vector containing the unknown coefficients v_{ji} mentioned in *(1)*, it may be shown that:

$$T = \frac{1}{2}\sum_{j=1}^{M}\sum_{k=1}^{M} v_{ji} Tjk\ v_{ki} = \frac{1}{2}\boldsymbol{v}_i^T[T]\boldsymbol{v}_i \quad ; \quad U = \frac{1}{2}\sum_{j=1}^{M}\sum_{k=1}^{M} v_{ji} Ujk\ v_{ki} = \frac{1}{2}\boldsymbol{v}_i^T[U]\boldsymbol{v}_i \tag{5}$$

With the aforementioned results, the last step in the Rayleigh-Ritz method is to find the vectors $\boldsymbol{v}_i$ such that the Rayleigh quotient R is minimized. As detailed by Shames [6], this is achieved by solving the following classical eigenvalues problem:

$$\min\{R\} = \min\left\{\frac{\boldsymbol{v}_i^T[T]\boldsymbol{v}_i}{\boldsymbol{v}_i^T[U]\boldsymbol{v}_i}\right\} \quad \Leftrightarrow \quad \det([U] - \omega_i^2[T]) = 0 \quad ; \quad ([U] - \omega_i^2[T])\boldsymbol{v}_i = \mathbf{0} \tag{6}$$

Solving *(6)* give the eigenfrequencies ω_i^2 characterizing the dry gate. Furthermore, the coefficients v_{ji} are also available and may then be introduced in *(1)* to get the dry modes shapes δ_i.

2.3. Dynamic Analysis

As soon as the eigenfrequencies of the dry structure are available, the next step in the seismic analysis is to determine the dynamic response of the lock gate and also the resulting hydrodynamic pressure acting on it. To so, we can follow the basic idea of the modal decomposition and assume that the out-of-plane displacements u characterizing the structure are expressed as a combination of the dry modes shapes δ_i calculated here above. In other words, we have:

$$u(y,z,t) = \sum_{j=1}^{N} q_j(t)\delta_j(y,z) \Leftrightarrow \delta u(y,z,t) = \sum_{k=1}^{N} \delta q_k(t)\delta_j(y,z) \tag{7}$$

where N is the total number of eigenmodes involved in the decomposition process and q_j are unknown time coefficients. These latter can be fixed by applying the virtual work principle. We may recall that, as explained by Jones [11], this theorem states that a necessary and sufficient equilibrium condition is that the internal and external virtual works have to be equal for any kinematically compatible displacements field. Consequently, if we want here to express the global equilibrium of the lock gate, we have to successively evaluate:

- The *internal work* δW_{int} associated to the deformations of the gate when this one is submitted to a virtual displacements field δu.
- The *external work* δW_{ext} done by all the forces acting on the structure for the virtual displacements field δu.

Let us start by evaluating δW_{int}. For an arbitrary compatible δu, this one is simply the sum of the virtual energies δW_p and δW_r dissipated to deform the plating and the reinforcing elements. These terms may be shown to be given by the following expressions:

$$\begin{aligned} \delta W_p &= D\int_0^H\int_0^l \left(\frac{\partial^2 u}{\partial y^2}\frac{\partial^2 \delta u}{\partial y^2} + \frac{\partial^2 u}{\partial z^2}\frac{\partial^2 \delta u}{\partial z^2} + \nu\frac{\partial^2 u}{\partial y^2}\frac{\partial^2 \delta u}{\partial z^2} + \nu\frac{\partial^2 \delta u}{\partial y^2}\frac{\partial^2 u}{\partial z^2} + 2(1-\nu)\frac{\partial^2 u}{\partial y\partial z}\frac{\partial^2 \delta u}{\partial y\partial z}\right)dydz \\ \delta W_r &= \sum_n EI_{h,n}\left[\int_0^l \frac{\partial^2 u}{\partial z^2}\frac{\partial^2 \delta u}{\partial z^2}dz\right]_{y\,=\,y_n} + \sum_n EI_{v,n}\left[\int_0^H \frac{\partial^2 u}{\partial y^2}\frac{\partial^2 \delta u}{\partial y^2}dy\right]_{z=z_n} \end{aligned} \tag{8}$$

If we now try to derive δW_{ext}, we have to account for all the forces acting on the gate during the earthquake. In the present paper, we will only consider the following ones:

- The *inertia forces* due to the total accelerations $\ddot{u} + \ddot{X}$. They are obtained by summing up the contributions coming from the plating and the reinforcing system:

$$-\int_0^H\int_0^l \rho t_p \delta u(\ddot{u} + \ddot{X})dydz - \sum_n \rho A_{h,n}\left[\int_0^l \delta u(\ddot{u} + \ddot{X})dz\right]_{y\,=\,y_n} - \sum_n \rho A_{v,n}\left[\int_0^H \delta u(\ddot{u} + \ddot{X})dy\right]_{z=z_n} \tag{9}$$

- The *damping forces* associated to the mass and the stiffness of the dry gate. For convenience, these ones will be simply designated by f_d but we will not provide here a detailed analytical expression to evaluate them (more details may be found in references [7] and [8] amongst others). It is worth noting that f_d is a force per unit of surface, so that the work performed for a given δu is:

$$-\int_0^H \int_0^l f_d(y,z,t)\delta u(y,z,t)dydz \tag{10}$$

- The *pressure forces* produced by the water surrounding the gate. As mentioned in the introduction, these ones are the sum of the convective, impulsive and flexible contributions. Nevertheless, if we assume that only the two latter are of importance, designating them respectively by p_r and p_f leads to the following expression for their virtual work:

$$-\int_0^{h_s} \int_0^l \big(p_r(y,t) + p_f(y,z,t)\big)\delta u(y,z,t)dydz \tag{11}$$

In this last equation, the rigid and flexible pressures p_r and p_f can be evaluated by using the closed-form solutions exposed by Kim [12] for example. We will not recall them here, but it is interesting to note that the time dependence of p_r is directly related to the seismic acceleration $\ddot{X}$, while the evolution of p_f is closely influenced by the accelerations $\ddot{u}$ of the gate. As a final remark concerning δW_{ext}, let us also mention that all the mathematical expressions *(9)*, *(10)* and *(11)* are affected with a minus sign as the external forces are always acting in the opposite sense of the virtual displacements δu.

The modal decompositions of u and δu given by *(7)* may now be introduced in *(8)*, *(9)*, *(10)* and *(11)* to get the unknown coefficients q_j. Doing so is quite fastidious but leads to the following results for δW_{int} and δW_{ext}:

$$\delta W_{int} = \sum_{k=1}^{N} \delta q_k \sum_{j=1}^{N} q_j K_{jk} \quad ; \quad \delta W_{ext} = -\sum_{k=1}^{N} \delta q_k \left[\sum_{j=1}^{N} \big(\ddot{q}_j M_{jk} + q_j(\alpha M_{jk} + \beta K_{jk}) - \ddot{q}_j J_{jk}\big) - P_k \ddot{X}\right] \tag{12}$$

in which α and β are the classical Rayleigh coefficients used respectively for the mass and stiffness proportional damping. Once again, for convenience, we will not provide here the detailed mathematical expressions for M_{jk}, K_{jk}, J_{jk} and P_k. Nevertheless, it is worth mentioning that M_{jk} and K_{jk} translates the effects of the mass and the stiffness of the gate, while J_{jk} and P_k are closely related to the flexible and rigid pressures.

Finally, if we equate δW_{int} and δW_{ext}, as the virtual work principle has to be satisfied for any δq_k, the results in *(12)* leads to a set of N equations that may be written under the following matrix form:

$$([M] - [J])\ddot{\boldsymbol{q}}(t) + (\alpha[M] + \beta[K])\dot{\boldsymbol{q}}(t) + [K]\boldsymbol{q}(t) = \boldsymbol{P}\ddot{X}(t) \tag{13}$$

in which q is a vector containing the unknown coefficients q_j. If the time evolution of the seismic ground acceleration $\ddot{X}$ is known, *(13)* can be solved by using the Newmark integration scheme to get the parameters q_j. These ones may then be introduced in *(7)* to evaluate the displacements and accelerations $\ddot{u}$ of the gate, which allows for the derivation of the flexible hydrodynamic pressure p_f.

As a final remark, it is worth noting that *(13)* is very closed to the classical equation translating the dynamic equilibrium of a structure submitted to the external forces $\boldsymbol{P}\ddot{X}$. Nevertheless, the fundamental difference here is the presence of the additional matrix $[J]$ in the left hand side of *(13)*. This term represents the action of the surrounding water and is responsible for a coupling between the gate and the fluid. If the pressure were calculated under the assumption of a perfectly rigid structure, then $[J]$ would not appear and *(13)* would be stricly equivalent to the equilibrium equation that is considered in the added-mass method as applied by Forsyth for example.

3. NUMERICAL VALIDATIONS

In order to check if the analytical approach exposed here above leads to satisfactory solutions, we can make some comparisons with the results obtained by performing modal and dynamic analyses with finite elements software. This is done for the developments of sections 2.2 and 2.3.

3.1. Description of the Structure

Let us start by presenting the particular structure that is used for the validations. A three dimensional view of the gate is presented on Figure 4. It is made of a single plating reinforced by six frames and five girders. All of them have a T-shaped cross-section with the properties listed in Table 2. Twenty smaller stiffeners are also present, mainly for preventing the plating from buckling. The dimensions of their rectangular cross-section are also given in Table 2. It is important to mention here that for convenience, the horizontal reinforcing elements are uniform over the height of the gate. In practice however, this is rarely the case as the gate is usually stiffer near the bottom of the lock. This particularity can of course be integrated in the present simplified analytical method because the cross-section properties $A_{h,n}$ and $I_{h,n}$ in equations *(3)*, *(4)*, *(8)* and *(9)* may be different for each element n.

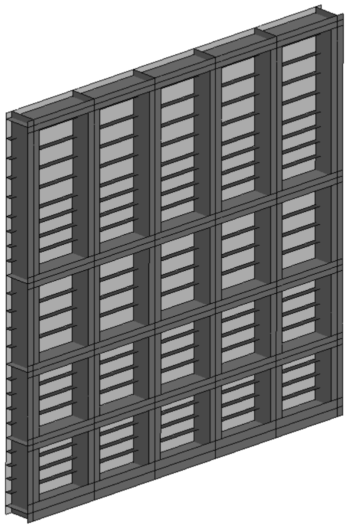

Figure 4: Three Dimensional View of the Gate

Table 1: Material Properties

Mass density	$\rho\ (kg/m^3)$	7850
Young modulus	$E\ (MPa)$	210000
Poisson ratio	ν (-)	0.3

The main distances between all the reinforcing components are presented on Figure 5. It can be seen that the frames are regularly spaced, but this is not the case for the girders and the stiffeners.

The gate is made of a linear elastic material characterized by a mass density ρ, a Young modulus E and a Poisson ration ν having the values listed in Table 1 and corresponding more or less to the properties of steel.

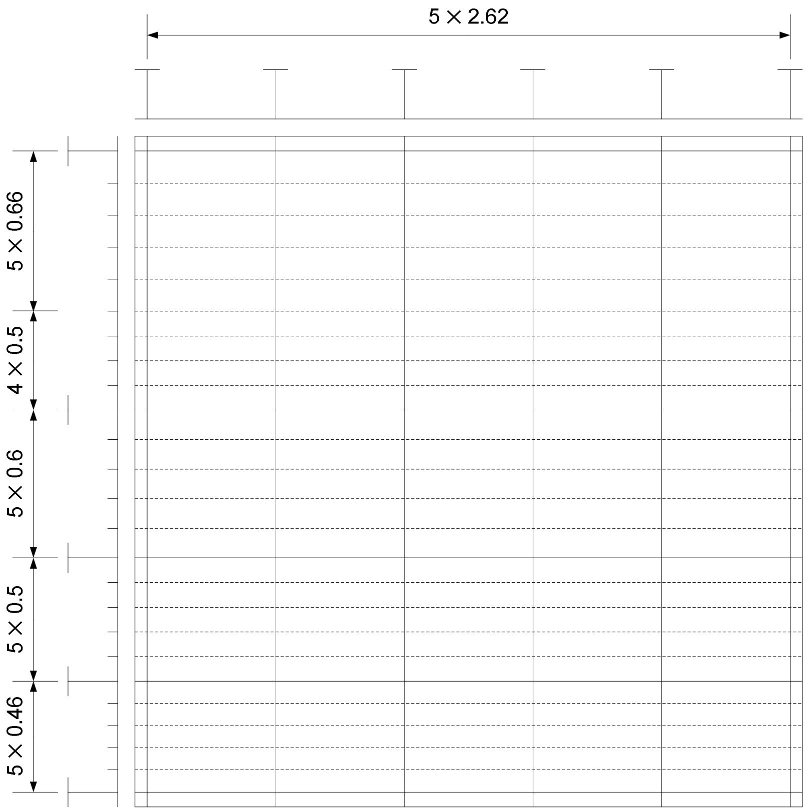

Figure 5: Main Distances (m) Between the Frames, the Girders and the Stiffeners

Table 2: Dimensions (m) of the Reinforcing System

Horizontal girders	
h_w	0.980
t_w	0.020
h_f	0.400
t_f	0.025
Vertical frames	
h_w	0.980
t_w	0.020
h_f	0.500
t_f	0.025
Horizontal stiffeners	
h_w	0.210
t_w	0.006
h_f	0.000
t_f	0.000

3.2. Numerical Validation of the Modal Properties

The aim of this section is to check the simplified prediction of the eigenfrequencies and mode shapes exposed in 2.2. To do so, we can compute numerically the modal properties of the gate described here above. This is achieved by using the software NASTRAN, in which the plating is modeled with isoparametric shell elements, while classical beam elements are used for the reinforcing system.

As expected for this kind of stiffened structure, the modal analysis performed with NASTRAN points out that the gate has only two dominant modes and a lot of local ones. Of course, the method detailed in section 2.2 is only able to capture the former, but hopefully, the latter do not have a lot of practical interest. Consequently, we simply have to check here that there is a satisfactory agreement on the modal properties for the two main global modes.

The natural frequencies derived numerically and analytically are listed in Table 3. An estimation computed by the finite elements software LS-DYNA is also presented. From these results, it transpires that the correlation is quite good, as there is only a maximal error of 7 % with the values calculated by LS-DYNA. The discrepancy with NASTRAN is a bit more important, as the error is reaching this time 11 %. Furthermore, it is interesting to note that our simplified approach tends to overestimate the eigenfrequencies. This is not really surprising, as it may be theoretically shown [6] that this is imputable to the Rayleigh-Ritz method.

Table 3: Eigenfrequencies Obtained Numerically and Analytically

Mode	Frequency (Hz)			Error (%)	
	NASTRAN	LS-DYNA	Analytical	NASTRAN	LS-DYNA
1	19.2	20.0	21.3	10.9	6.5
2	23.3	25.3	26.0	11.6	2.7

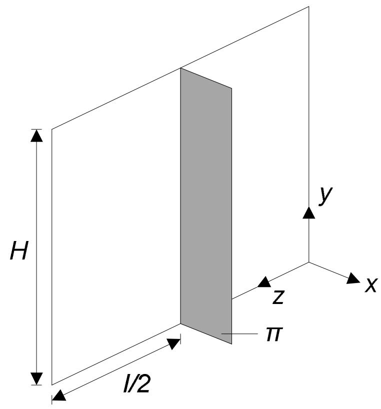

Figure 6: Definition of Plane *π* for Comparing the Modes Shapes

The second step is now to check if there is also a close agreement on the eigenmodes. To do so, we can compare the modes shapes in the vertical plane π that is perpendicular to the gate and crossing it in the middle (i.e. in $z = l/2$), as depicted on **Erreur ! Source du renvoi introuvable.**. The obtained results are depicted on Figure 7. Here again, we see that the agreement is also satisfactory.

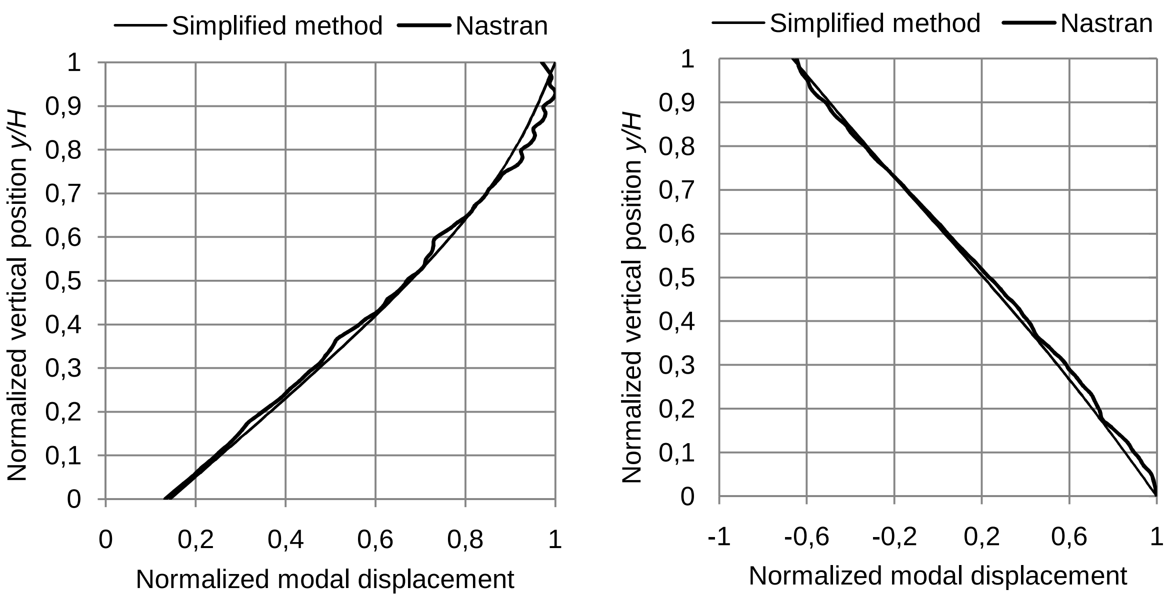

Figure 7: Comparison of the First and Second Eigenmodes Obtained Numerically and Analytically

As a conclusion, it transpires from the results exposed here above that the present simplified method leads to a pretty good approximation of the modal properties of the gate. The next phase is then to check that this also the case if the gate is submitted to an earthquake.

3.3. Numerical Validation of the Hydrodynamic Pressure

Let us now try to validate the analytical developments performed in section 2.3. The goal here is to check if our rapid prediction of the total hydrodynamic pressure induced on a lock gate during a seism is more or less closely correlated to the one derived numerically.

To do so, we consider a lock chamber having a total length L of $50\ m$, filled with water up to a level h_s of $8\ m$ (Figure 1) and submitted to the longitudinal seismic acceleration $\ddot{X}$ of Figure 8.

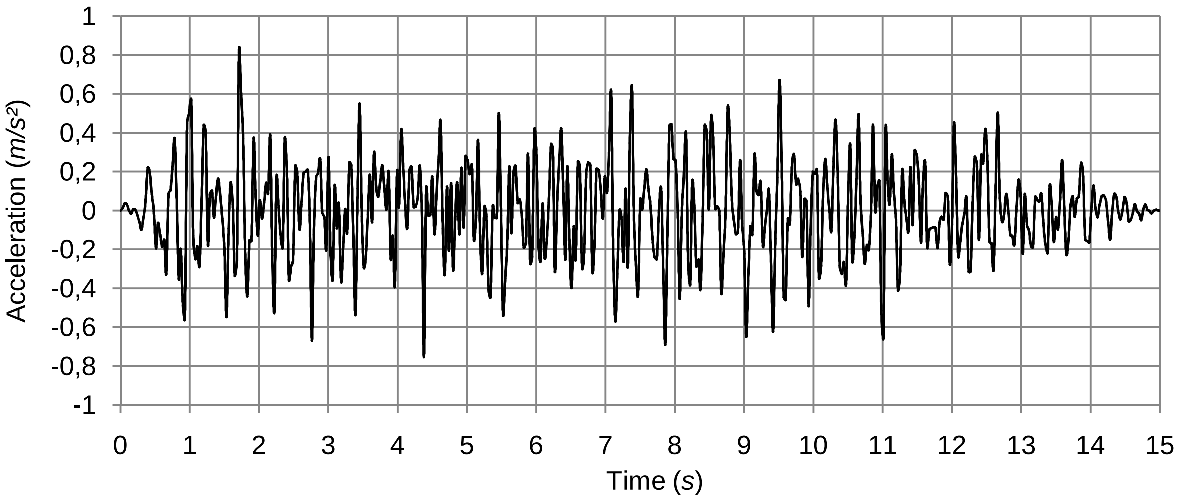

Figure 8: Time evolution of the longitudinal acceleration Ẍ applied to the gate

The numerical simulation is performed using the software LS-DYNA. In order to simulate the interaction between the gate and the water, it is required to have a finite elements model of both of them. In this article, constant stress solid elements [14] are used for the liquid, which means that the water is considered as an elastic medium with no shearing. The mesh of the fluid domain is regular, with a size of $20 \times 20 \times 20\ cm$ (Figure 9).

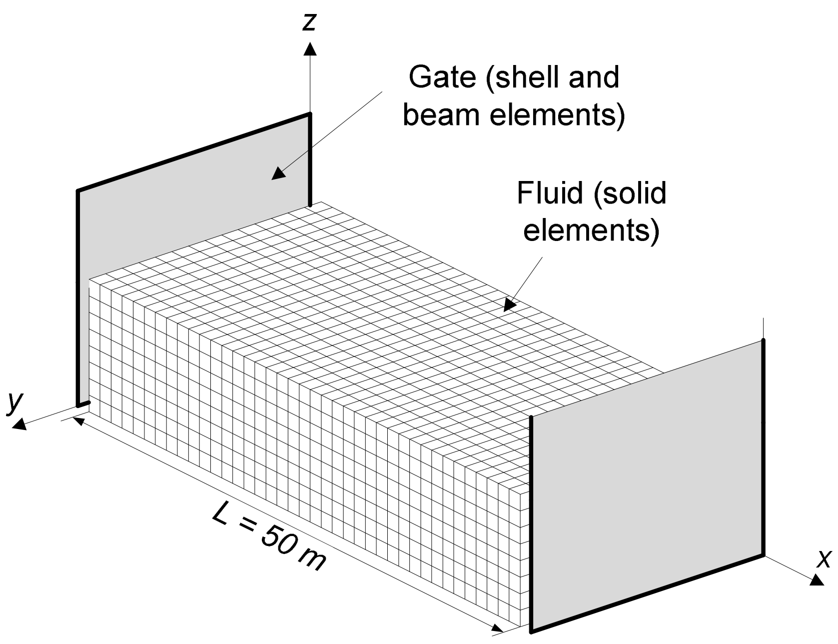

Figure 9: Finite Elements Model for the Dynamic Simulations

On Figure 9, the upstream and downstream gates are assumed to be the same as the one presented in section 3.3 (see Figure 4, Figure 5 and Table 2 for more details). The plating is model with

Belytscko-Tsay shell elements [14], while Hughes-Liu beams [14] are used for the stiffening components. The material is still linear elastic, with the properties of Table 1.

It is worth mentioning that the fluid and the structure do not share any nodes. In other words, the liquid is free to slide on the gate, friction beeing of course prohibited. To prevent the fluid from passing through the structure, the LS-DYNA contact algorithm is used for simulating the contact between the two entities.

In order to check the validity of the pressures derived analytically through the simplified dynamic analysis of section 2.3, we can make a comparison of the total resulting hydrodynamic force F applied on the strucutre. This one is simply obtained by integrating the rigid and flexible contributions p_r and p_f over the entire surface of the gate, i.e.:

$$F(t) = \int_0^{h_s} \int_0^{l} \big(p_r(y,t) + p_f(y,t)\big) dy dz \tag{14}$$

The time evolutions of F predicted analytically and calculated by LS-DYNA are plotted on Figure 10, for the seismic accelaration of Figure 8. We see that there is a quite good agreement between the two curves.

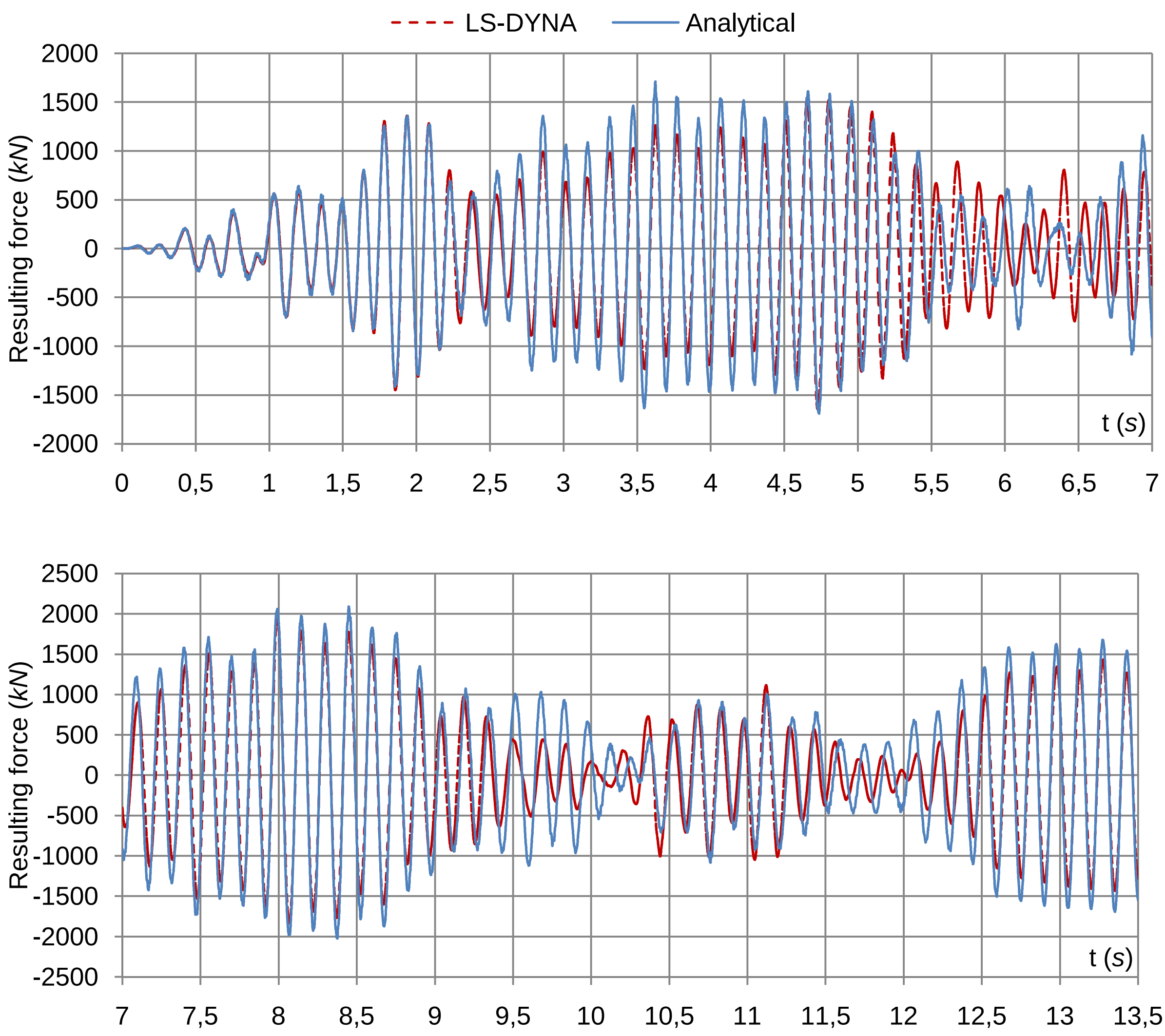

Figure 10: Time Evolution of the Total Hydrodynamic Force Applied on the Gate

Moreover, we may also points out that the present simplified method tends to provide a conservative evaluation of the pressures, which is. Indeed, if we look at the extreme values listed in Table 4, we see that the analytical solution is overestimating the maximal value by an amount of $8\,\%$ more or less, while the minimal one is underestimated by $10\,\%$.

Table 4: Extreme Values of the Total Hydrodynamic Force Appearing During the Earthquake

	Analytical solution F_T	Numerical solution F_N	Rigid solution F_R	Relative difference $\|1 - F_T/F_N\|$	Ratio F_T/F_N
Maximal value	$2085.4\ kN$	$1936.1\ kN$	$375.2\ kN$	7.7 %	5.2
Minimal value	$-2020.8\ kN$	$-1834.2\ kN$	$-517.1\ kN$	10.2 %	3.9

Another point that is interesting to investigate is the importance of accounting for the structure flexibility when evaluating the pressures. If the gates were perfectly rigid, then only the contribution p_r would be acting on them. Integrating p_r over the entire surface of the gate leads to the rigid total hydrodynamic force F_R:

$$F_R(t) = l \int_0^{h_s} p_r(y,t)dy \tag{15}$$

The extreme values of F_R are also listed in Table 4. If we further look at the ratios of the following extreme values:

$$\frac{\max\limits_t\{F(t)\}}{\max\limits_t\{F_R(t)\}} \quad ; \quad \frac{\min\limits_t\{F(t)\}}{\min\limits_t\{F_R(t)\}} \tag{16}$$

we see from the rightmost column of Table 4 that assuming a perfectly rigid gate leads to a maximal resulting force five times smaller than the one computed numerically. Similarly, the minimal value is underestimated by a factor four. Of course, designing a lock gate with these results is not acceptable, which shows the real need of considering the structure flexibility.

4. CONCLUSION

The first part of this paper presents a simplified analytical procedure allowing for a rapid estimation of the modal properties of a lock gate with a single plating and an orthogonal stiffening system. The natural frequencies and mode shapes provided by this approach are compared to those given by the finite elements software NASTRAN for a given lock gate. The agreement between the analytical predictions and the numerical solutions are found to be satisfactory, which tends to corroborate our developments.

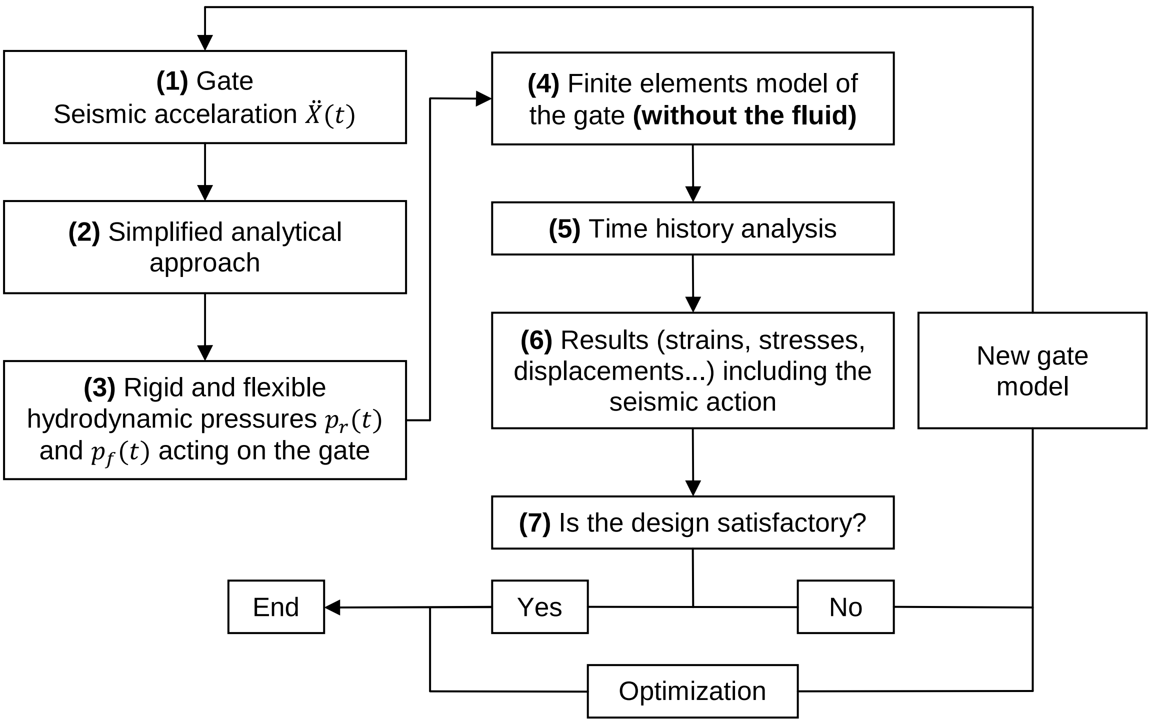

Figure 11: Flow Chart of the Pre-Design Process Including the Seismic Action

In the second part of the article, a consistent method is also exposed to perform a simplified dynamic analysis of a lock gate submitted to an earthquake. This allows for an estimation of the hydrodynamic pressures acting on the gate during the seism. These developments were also validated by making a comparison with solutions given by the finite elements software LS-DYNA.

The practical interest of the exposed method is to provide a very quick way for estimating the time evolution of the rigid and flexible pressures p_r and p_f. This may help the engineers to integrate the seismic action in the design process. Indeed, let us consider the flow-chart depicted on Figure 11. For a given lock gate submitted to a longitudinal acceleration $\ddot{X}$, we can use this simplified approach to rapidly get the time evolution of p_r and p_f. These pressures may then be included in a finite elements model of the gate,in which there is no need to model the fluid domain as its action is already accounted for by applying p_r and p_f on the structure. A time history analysis of the gate submitted to $\ddot{X}$, p_r, p_f and all the other required actions (hydrostatic pressure, damping forces...) leads to the extreme values of the stresses, strains and displacements. If the design is not satisfactory, then a reinforcement is necessary and the process of Figure 11 is started again. On the other hands, if the design is sufficient, then the process may be stopped or started again for optimization.

Consequently, the method of Figure 11 shows that there is no need to model the fluid domain while performing finite elements analyses. This considerably reduces the complexity of preliminary seismic analyses of lock gates. All these achievements are likely to help engineers in integrating the seismic action when pre-desingning lock gates. Nevertheless, this conclusion has to be nuanced, as one has always to bear in mind that the present approach is based on some simplifying assumptions (for example, the support conditions of the gate are somewhat idealized). For this reason, working with a refined model of the structure is still required, but only at the very last step of the design process.

5. REFERENCES

[1] Haroun M.A. (1984). Stress Analysis of Rectangular Walls Under Seismically Induced Hydrodynamic Loads, Bulletin of Seismological Society of America, 74(3), 1031-1041.

[2] Housner G.W.(1974). Dynamic Pressures on Accelerated Fluid Containers, Bulletin of Seismological Society of America, 47(1), 15-37.

[3] Ibrahim R.A. (2005). Liquid Sloshing Dynamics: Theory and Applications, Cambridge University Press.

[4] Epstein H.I. (1976). Seismic Design of Liquid Storage Tanks, Journal of the Structural Division, 102(9), 1659-1673.

[5] Westergaard H.M. (1933). Water Pressure on Dams During Earthquakes, Transactions of the American Society of Civil Engineers, 98(2), 418-433.

[6] Shames I.H. & Dym C.L. (1995). Energy and Finite Element Methods in Structural Mechanics, New Age International.

[7] Zeng H. & Bert C.W. (2001). Free Vibration Analysis of Discretely Stiffened Skew Plates, International Journal of Structural Stability and Dynamics, 1(1), 125-144.

[8] Amiri S.N. & Esmaeily A. (2010). Prediction of Dynamic Response of Stiffened Rectangular Plates Using Hybrid Formulation, Journal of Engineering Science and Technology, 5(3), 251-263.

[9] Iyengar K.T. & Narayana R. (1967). Determination of the Orthotropic Plate Parameters of Stiffened Plates and Grillages in Free Vibration, Applied Sciences Research,17(6), 422-438.

[10] Leissa A.W. (1973). The Free Vibration of Rectangular Plates, Journal of Sound and Vibration, 31(3), 257-293.

[11] Jones N. (2003). Structural Impact, Cambridge University Press.

[12] Kim J.K., Koh K.H. & Kwahk I.J. (1996). Dynamic Response of Rectangular Flexible Fluid Containers, Journal of Engineering Mechanics, 122(9), 807-817.

[13] Forsyth G. & Porteous A. (2000). The Design and Construction of Seismically Qualified Steel Caissons at Rosyth Royal Dockyard, The Structural Engineer, 78(21), 24-31.

[14] Hallquist J.O. (2006). LS-DYNA Theoretical Manual, Livermore Software Technology Corporation.